Bioorganic & Medicinal Chemistry 17 (2009) 6040–6047

Contents lists available at ScienceDirect

Bioorganic & Medicinal Chemistry

journal homepage: www.elsevier.com/locate/bmc

Design, synthesis, and discovery of novel non-peptide inhibitor of Caspase-3 using ligand based and structure based virtual screening approach

P. Jhansi Lakshmi [a], B. V. S. Suneel Kumar [b], Ravi Shasi Nayana [b], M. Srinivas Mohan [a], Ramababu Bolligarla [c], Samar K. Das [c], M. Uday Bhanu [d], Anand K. Kondapi [d], Muttineni Ravikumar [b,*]

[a] Department of Chemistry, Osmania University College for Women, Koti, Hyderabad 5000095, India
[b] BioCampus, GVKBIO Sciences Private Limited, S-1, Phase-1, TIE, Balanagar, Hyderabad 500037, India
[c] School of Chemistry, University of Hyderabad, Hyderabad 500046, India
[d] Department of Biotechnology, University of Hyderabad, Hyderabad 500046, India

ARTICLE INFO

Article history:
Received 14 February 2009
Revised 22 June 2009
Accepted 23 June 2009
Available online 7 July 2009

Keywords:
Caspase-3
Virtual screening
Pharmacophore
Docking
Apoptosis

ABSTRACT

Caspase-3 belonging to a family of cysteine proteases is main executioner of apoptotic cascade pathway. The inhibitors of this protein are useful in the treatment of cardiomyopathy and neurodegenerative diseases. For the discovery of novel Caspase-3 non-peptide inhibitors from Maybridge database, ligand based and structure based virtual screening methods were used. Quantitative 3D pharmacophore models were generated using 25 known inhibitors of Caspase-3 and it was used as initial screen to retrieve the hits from the database. These compounds with high estimated activity were analyzed for drug like properties and docking studies were performed, to study the interaction between new hits and active site. One of the hits (AW01208), with good predictions was selected for synthesis and biological screening. This compound showed an inhibition activity against Caspase-3 in SKNH cell lines.

1. Introduction

Caspases are a family of cysteine proteases responsible for promoting cell death (Apoptosis).[1] Caspase-3 (apopain), is situated at a key junction in the apoptosis, mediating apoptotic cascade from the intrinsic and extrinsic activation pathways. Apoptosis has been observed in a large number of pathological conditions, including ischemia-reperfusion injury (stroke and myocardial infarction), cardiomyopathy, neurodegeneration (Alzheimer's disease, Parkinson's disease, Huntington's disease, and ALS), sepsis, type I diabetes, and allograft rejection.[2,3] Two different classes of caspases involved in apoptosis, the initiator caspases and the executioner caspases. The initiator caspases, which include Caspase-2, -8, -9, and -10, are located at the top of the signalling cascade; their primary function is to activate the executioner caspases, Caspase-3, -6, and -7.

The executioner caspases are responsible for the physiological (e.g., cleavage of the DNA repair enzyme poly (ADP-ribose) polymerase-1, nuclear laminins, and cytoskeleton proteins) and morphological changes (DNA strand breaks, nuclear membrane damage, and membrane blebbing) that occur in apoptosis. Most of the caspases are activated by cleavage at a specific aspartate site by assembly of their active subunit forms. Activation of Caspase-9 requires the release of cytochrome *c* from mitochondria to cytosol where the caspase resides. Caspase-3 is activated by the upstream Caspase-8 and Caspase-9 and since it serves as a convergence point for different signalling pathways.[4,5]

Several Merck Caspase-3 inhibitors are currently in preclinical trials. M-826, a small reversible Caspase-3 inhibitor, blocked brain tissue damage in an animal model of hypoxia–ischemia when injected 2 h after ligation[6] and another merck Caspase-3 specific inhibitor M-791 decreased lymphocyte apoptosis in thymus and spleen of mice subjected to sepsis induced by cecal ligation-puncture and rescued 80–90% of animals from lethal septic shock.[7,8]

In our present study, we used computational approach to identify the potent and selective Caspase-3 inhibitors. Three-dimensional (3D) pharmacophore models were generated using the known set of Caspase-3 inhibitors, to reveal the chemical features required for its activity. Best pharmacophore (Hypo 1) is validated with docking and structure based pharmacophore studies. These models were used to rapidly screen compounds from Maybridge database, for the identification of a series of novel and highly potent Caspase-3 inhibitors. Ten molecules were selected from virtual screening using pharmacophore as query and these molecules are selected for synthesis and in vitro screening studies based on the docking scores, predicted binding location and their drug like properties.

* Corresponding author. Tel.: +91 9989889074.
E-mail address: ravambio@gmail.com (M. Ravikumar).

0968-0896/$ - see front matter © 2009 Elsevier Ltd. All rights reserved.
doi:10.1016/j.bmc.2009.06.069

2. Methods

2.1. Molecular modelling

We have collected 97 human Caspase-3 inhibitors with activity data (IC_{50}) spanning over 6 orders of magnitude (from 0.1 nM to 27,900 nM)[9–15] from research articles. Activity measured was at same assay method for all the compounds used in this study. Activity values are uniformed to nM. The 3D structures of all molecules were constructed by using Cerius2[16] and further these molecules are subjected to energy minimization using the steepest descent algorithm with a convergence gradient value of 0.001 kcal/mol. The Geometry optimization was carried out with the MOPAC 6 packages using semi empirical AM1 Hamiltonian method.[17]

2.2. Pharmacophore generation

Pharmacophore models were generated for known inhibitors of Caspase-3 using Catalyst package.[18] Chemical-featured quantitative pharmacophore can be generated automatically using the HypoGen module within Catalyst, provided that structure–activity relationship data of a well-balanced set of compounds is available.

All compounds used in the study were subjected to best method option of conformational search using Monte Carlo-like algorithm together with poling[19] to generate a maximum of 250 conformers. Our models emphasized a conformational diversity within the constraint of a 20 kcal/mol energy threshold above the estimated global minimum based on use of the CHARMM force field and using poling algorithm.[20,21] The molecules associated with their conformation models were then submitted to Catalyst hypotheses generation.

The dataset was divided into training set and test set, considering both structural diversity and wide coverage of the activity range (shown in Scaffold 1–5, in Supplementary data). The compounds with activity with <10 nM were considered as highly actives (+++), compounds with an activity range of 10–100 nM as moderate actives (++) and activity of >1000 nM as least actives (+).

In hypotheses generation, the structure and activity correlations in the training set were rigorously examined. HypoGen identifies features that are common to the active compounds but excludes common features for the inactive compounds within conformationally allowable regions of space. Ten hypotheses were generated for every HypoGen run from which the ones with the highest correlation values were chosen. The pharmacophore models were validated using cost analysis and test set activity prediction.

The best pharmacophore (Hypo 1) having high correlation coefficient (r), lowest total cost, and lower RMSD value was chosen to estimate the activity of test set (Details of Cost parameters mentioned in Supplementary data).

2.3. Docking studies

X-ray crystal structure of Caspase-3 (PDB ID 1pau with a resolution of 2.50 Å) was used for docking studies. Preparation of the protein for docking included removal of ligand and solvent coupled with addition of hydrogen atoms. All selected inhibitors were docked into the active site of the target protein using Glide (version 8.0, Schrödinger, Inc.) in standard precision mode (Glide SP).[22,23] The binding region was defined by a 12 A^0_12 A^0_12 A^0 box centred on the centroid of the crystallographic ligand to confine the centroid of the docked ligand. No scaling factors were applied to the Van der Waals radii. Default settings were used for all the remaining parameters. The top 20 poses were generated for each ligand. The docking poses were then energy minimized with Macro model in the OPLS2001 force field[24] with flexible ligand and rigid receptor. Best pose was selected on the basis of Glide score and the interactions formed between the ligands and active site amino acids.

2.4. Virtual screening

To find the novel non-peptide inhibitors of Caspase-3, virtual screening was conducted on Maybridge database[25] containing about 50,000 compounds along with their conformations. Best pharmacophore model (Hypo 1) comprising of four chemical features was used as a query to retrieve the leads from the database. Fast flexible search method was used for database searching to retrieve new lead molecules.

2.5. Experimental

In silico studies led to the identification of top 10 lead compounds with Caspase-3 inhibitor activity. The synthesis of AW01208 (3,4-dichloro-*N*-{3-[4-(2-chloro-6-fluoro-benzyl)-piperazin-1-yl]-propyl}-benzamide) is described in-detail in Scheme 1. Spectral data such as NMR, IR, and LC–MS of AW01208 was given in Scheme 2 (Supplementary data). After synthesis, the lead compound AW1208 (3,4-dichloro-*N*-{3-[4-(2-chloro-6-fluoro-benzyl)-piperazin-1-yl]-propyl}-benzamide) was used to carry out in vitro bioassay studies using spectroflourimetric techniques to assess the Caspase-3 inhibition ability of the synthesized compound. All chemicals and reagents were purchased from Aldrich Chemical Co. unless and otherwise indicated, and used without further purification. All reactions were carried out under an inert nitrogen atmosphere with dry solvents using anhydrous conditions unless otherwise stated. The ^1H NMR spectra of compounds were recorded on Bruker DRX-400 spectrometer using $Si(CH_3)_4$ [TMS] as an internal standard. Samples were dissolved in an appropriate deuterated solvent ($CDCl_3$). Proton chemical shifts are reported as parts per million (δ) relative to tetramethylsilane (Me_4Si; 0.00 ppm), ^{13}C NMR spectra are reported as δ relative to deuterated chloroform ($CDCl_3$, 77.0 ppm). Solution mass spectrum (LCMS) of compound AW01208 was obtained on a LCMS-2010A Shimadzu spectrometer using ESI mode of ionisation. Infrared (IR) spectra were recorded on KBr pellets with a JASCO FT/IR-5300 spectrometer in the region of 400–4000 cm^{-1}

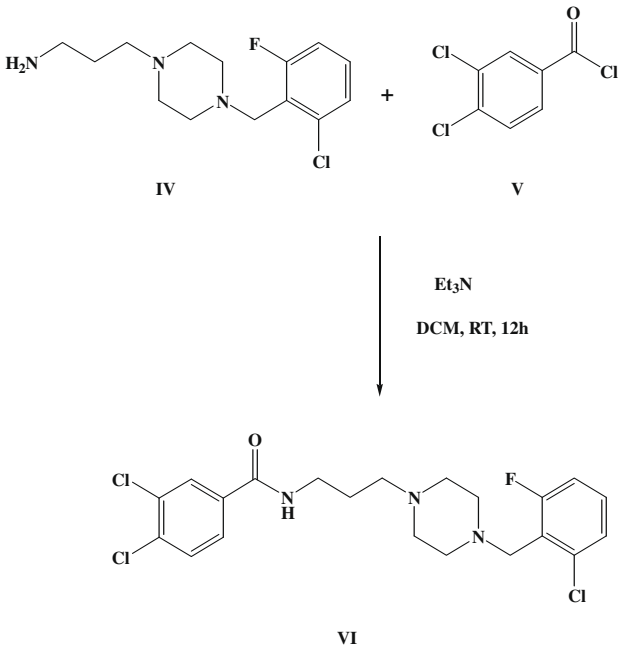

2.5.1. Synthesis of (3-bromopropyl) carbamic acid benzyl ester (II)

The compound was prepared according to the literature.[26]

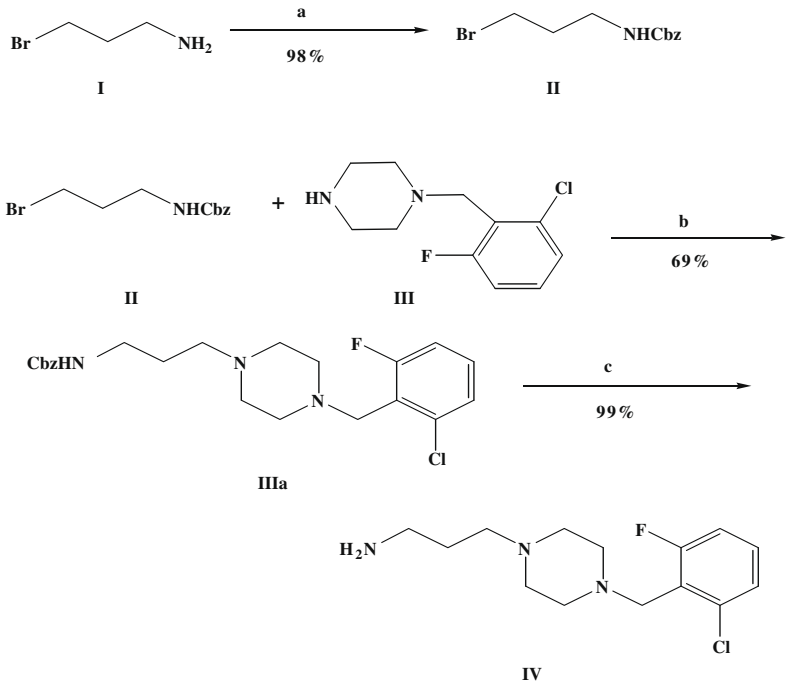

Scheme 1. Reagents and conditions: (a) benzylchloroformate; (b) K_2CO_3, MeCN, 80 °C; (c) iodotrimethysilane, MeCN.

2.5.2. Synthesis of {[3-(4-(2-chloro, 6-fluoro benzyl piperazin-1-yl)] propyl} carbamic acid benzyl ester (IIIa)

The free base (**III**) form of (**IIIa**) (0.450 g) and the alkyl bromide (0.650 g) (1.1 equiv) and K_2CO_3 (0.78) (2 equiv) were heated to reflux in 20.0 mL CH_3CN solvent for 4 h under nitrogen atmosphere. The mixtures were cooled at room temperature. Then evaporated the solvent and the residue dissolved in water and extracted with ethyl acetate. The organic extract was dried (Na_2SO_4) filtered and solvent evaporated in vacuo to give the product as clear oil. Column chromatography (100% ethyl acetate, R_f 0.4). NMR data: ^{1}H NMR (400 MHz, δ ppm) ($CDCl_3$): 1.62–1.68 (m, 2H), 2.40–2.58 (br d, 10H), 3.26 (q, 2H, J = 4.6 Hz), 3.70 (s, 2H), 5.09 (s, 2H), 5.89 (s, 1H), 6.95–6.99 (m, 1H), 7.18 (s, 2H), 7.28–7.30 (m, 5H).

2.5.3. Synthesis of {[3-(4-(2-chloro, 6-fluoro benzyl piperazin-1-yl)] propylamide (IV)

Iodotrimethylsilane (0.278 mL, 1.94 mmol) was added to a solution of compound (**IIIa**) (0.278 g, 1.94 mmol) in acetonitrile (5 mL). The reaction mixture was stirred for 15 min at room temperature, quenched with methanol (3 mL) and stirred for an additional 10 min. Volatiles are removed in vacuo; the residue was dissolved in 3 N HCl (10 mL) and extracted with ether (6.0 mL). The aqueous portion was neutralized to pH 9–10 with aqueous NH_4OH. Extraction with $CHCl_3$ (5.0 mL) and drying (Na_2SO_4) followed by evaporation yielded the product as a clear viscous oil that was used in the next step without further purification. NMR and IR data: ^{1}H NMR (400 MHz, δ ppm) ($CDCl_3$): 1.60–1.66 (m, 2H), 2.38 (t, 2H, J = 7.4 Hz), 2.46 (br s, 4H), 2.60 (br s, 4H), 2.74 (t, 2H, J = 6.8 Hz), 3.73 (s, 2H), 6.93–6.70 (m, 1H), 7.17–7.19 (m, 2H). ^{13}C NMR δ 30.29, 40.79, 52.30, 52.61, 53.23, 56.41, 113.9, 123.7, 125.37, 129.05, 136.63, 160.86. IR (NaCl plate, neat) 697, 1134, 1260, 1538, 1694, 2946, 3332 cm^{-1}.

2.5.4. Synthesis of 3,4-dichloro-*N*-{3-[4-(2-chloro-6-fluoro-benzyl)-piperazin-1-yl]-propyl}-benzamide (VI)

A mixture of amine (**IV**) (0.15 mL) (1 equiv), triethylamine and 5.0 mL dry DCM was stirred under nitrogen gas for 10 min, then the acid chloride (**V**) (0.080 g) (1.1 equiv) was added and stirred continuously for 12 h. The solvent was removed under reduced pressure and mixture was stirred with water. Later extracted into ethyl acetate and the organic layer washed with water and brine solution then with water and dried with Na_2SO_4. The solvent was evaporated by rotary vapour and separated by the column chromatography by using 4% methanol + 96% $CHCl_3$ mixture. A clear oily liquid compound was obtained. NMR data: ^{1}H NMR (400 MHz, δ ppm) ($CDCl_3$): 1.92 (s, 2H), 2.76 (br d, 8H), 3.48 (s, 2H), 3.69 (s, 2H), 4.04 (br s, 2H), 6.93 (d, 1H), 7.15 (s, 1H), 7.39 (d, 1H), 7.72 (d, 1H), 7.99 (s, 1H), 8.40 (s, 1H). Mass spectra given in SI, LCMS Data: Molecular ion peak obtained at 458 with few other fragment peaks.

2.6. Biological screening

Caspase-3 inhibition studies were estimated by using a Spectrofluorometric method[27,28] by measuring the accumulation of a flourogenic product. The activities of the compound were evaluated in SKNSH cell lines as a cell-based model of apoptosis. The compound inhibited Caspase-3 activity in a concentration dependent manner.

Inhibition studies were carried out using Caspase-3 Assay kit (BD Pharmingen™). The kit is designed to measure Caspase-3 cleaving activity, an early marker of cells undergoing apoptosis. Doxorubicin induced apoptotic extracts were used as Caspase-3 and 7 sources. Ac-DEVD-AMC is a synthetic tetra peptide flourogenic substrate (MW = 675 Da; purity $\geq$ 98%) that was used to identify and quantitate Caspase-3 activity in apoptotic cell lysates.

Caspase-3 cleaves the tetra peptide between D and AMC, releasing AMC. The enzymatic activity of Caspase-3 and 7 was determined by measuring the accumulation of the flourogenic product 7-amino-4-methyl coumarin (AMC) using an excitation wavelength of 380 nm and an emission wavelength range of 420–460 nm. Apoptotic cell lysates containing active Caspase-3 yield a considerable emission as compared to non-apoptotic cell lysates. The Caspase-3 and 7 were first assayed to determine the optimal

concentration for each experiment. Optimal concentrations were based in the linear range of the enzyme activation curves.

The Caspase-3 protein inhibitor compound was tested with the standard compounds as a control for caspase activity. The non-peptide inhibitor was dissolved in DMSO, and a serial dilution was performed before screening in order to obtain desired concentrations. The compound synthesized was analyzed for Caspase-3 inhibitory activity with doxorubicin induced extract for Caspase-3 source.

3. Results and discussion

3.1. Pharmacophore generation

Pharmacophore models are developed in HypoGen module in Catalyst software. All dataset compounds were divided into a training set of 25 compounds and a representative test set of 72 compounds. HypoGen attempts to construct the simplest hypotheses that best correlates the activities (experimental vs predicted).

Ten statically best pharmacophore models were generated and these models were considered for further analysis. The Null cost (no correlation cost) for 10 hypotheses was 173.02, the fixed cost (ideal cost) of the run was 100.12 and the configuration cost was 14.90. A difference of 59.45 bits obtained between fixed and null costs is a sign of highly predictive nature of hypotheses. All 10 hypotheses generated showed high correlation coefficient between experimental and predicted IC_{50} values, in the range of 0.93–0.86 and moreover, these are having cost difference greater than 45 bits between the cost of each hypothesis and the null cost. It indicates that all the hypotheses are having true correlation between 75% and 90%. The cost values, correlation coefficients (r), RMSD, and pharmacophore features are listed in Table 1. The best pharmacophore (Hypo 1) consisted of one H-bond acceptor (HBA), one H-bond donor (HBD), and two hydrophobic (HY) features shown in Figure 1. This model is having high correlation coefficient (r) of 0.93, lowest total cost (59.45), and least RMSD value (0.98) and it was chosen to further validate its predictive power by estimating the activity of test set.

For the highly active compound (62) all the features are perfectly mapped to the features of Hypo 1 and had a fit score of 9.19, shown in Figure 2a. Whereas, for the least active compound (92) only three features of Hypo 1 were mapped properly and had fit value of 4.98, shown in Figure 2b. In compound 62, HBA feature is mapped to oxygen atom of carbonyl group present in amide moiety. The HBD feature mapped to the NH group which is attached to the 5th position of 4-oxo pentanoic acid. Among the two hydrophobic groups, one was mapped to the tertiary butyl group substituted at 5th position on pyrazine ring of the compound and another on *n*-pentane chain.

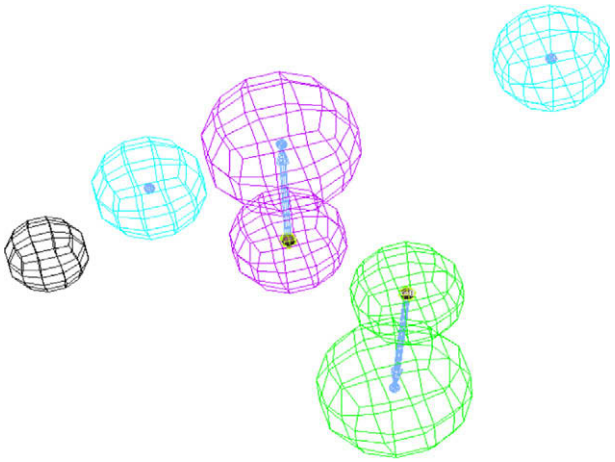

Figure 1. The best hypothesis model Hypo 1 produced by the HypoGen module in Catalyst 4.11 software. Pharmacophore features are color-coded with green, blue, and red contours representing the hydrogen-bond acceptor feature (A), hydrophobic feature (Z), hydrogen bond donor, respectively. Distance between pharmacophore features are reported in angstroms (Å).

The experimental and predicted activities of training set are listed in Scaffold 1–5 (in Supplementary data). In training set, among the 7 highly active compounds, all are predicted as highly active (+++). Out of 8 moderately active compounds (++), only three compounds was predicted as high active (+++), and the rest were predicted on the target. Out of 10 least active compounds, all compounds were predicted as least active (+).

The prediction power of Hypo 1 was evaluated by using 72 test set containing chemically diverse compounds. The experimental and predicted activities of test set are listed in str1–5 (in Supplementary data). Among the 9 highly active '+++' compounds in the test set, pharmacophore model was able to predict 8 compounds correctly and only one compound predicted as moderate active. Out of 47 compounds present in moderately active '++' range, 39 compounds predicted as '++', but 7 compounds predicted as high active and one compound inactive. Out of 16 least actives only 3 compounds predicted as '++'.

For the highly active compound (97) all the features are perfectly mapped to the 3 features of Hypo 1, shown in Figure 2a. Whereas, for the least active compound (11) mapped three features of Hypo 1 were mapped properly, shown in Figure 3b.

The generated pharmacophore model has predicted the activity of these test set compounds with correlation of 0.88 (shown in Graph 1). The over all correlation between the experimental and predicted activity was about 0.88 and hence from this analysis, Hypo 1 was able to distinguish actives from the inactives.

Table 1
Results of pharmacophore hypothesis generated using training set against Caspase-3 inhibitors

Hypo no.	Total cost	Cost-difference	Error cost	RMS	Correlation	Features
1	113.57	59.45	96.24	0.98	0.93	A,D,H,H
2	115.78	57.24	97.96	1.05	0.92	A,D,H,H
3	118.02	55.00	100.76	1.15	0.90	A,D,H,H
4	118.11	54.91	101.51	1.18	0.89	A,D,H,H
5	120.20	52.82	103.23	1.23	0.88	A,D,H,H
6	121.09	51.93	104.96	1.29	0.87	A,D,H,H
7	121.31	51.71	104.55	1.27	0.87	A,D,H,H
8	121.80	51.22	105.40	1.30	0.87	A,D,H,H
9	122.15	50.87	105.25	1.30	0.87	A,D,H,H
10	122.16	50.86	105.84	1.31	0.86	A,D,H,H

All cost values are in bits.
A = hydrogen bond acceptor, D = hydrogen bond donor, H = hydrophobic.
Cost details of ten pharmacophores: Fixed cost: 100.12, Configuration cost 14.90 and Null cost 173.02.

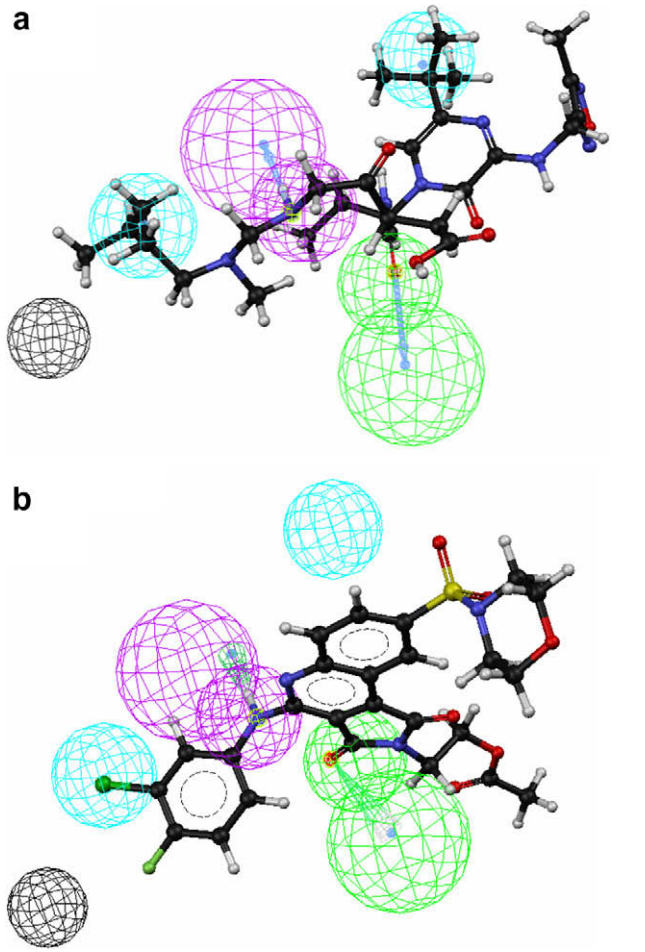

Figure 2. Pharmacophore mapping of the most active and least compound (1 from the training set) on the best hypothesis model Hypo 1 (a). Pharmacophore mapping of the highest active compound on the best hypothesis model Hypo 1 from the training set model number 62. (b) Pharmacophore mapping of the least active compound on the best hypothesis model Hypo 1 from the training set model number 92.

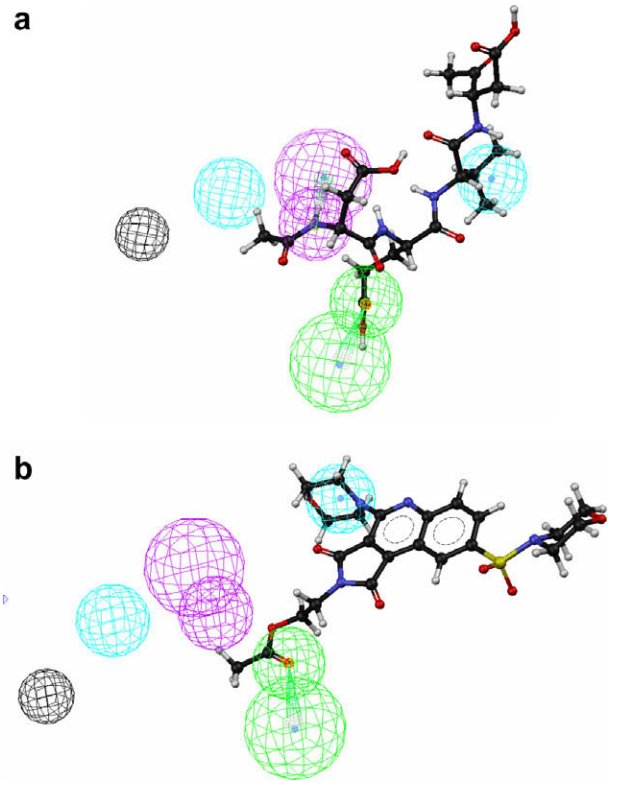

Figure 3. Pharmacophore mapping of the most active and least compound (1 from the test set) on the best hypothesis model Hypo 1 (a). Pharmacophore mapping of the highest active compound on the best hypothesis model Hypo 1 from the test set model number 77. (b) Pharmacophore mapping of the least active compound on the best hypothesis model Hypo 1 from the test set model number 91.

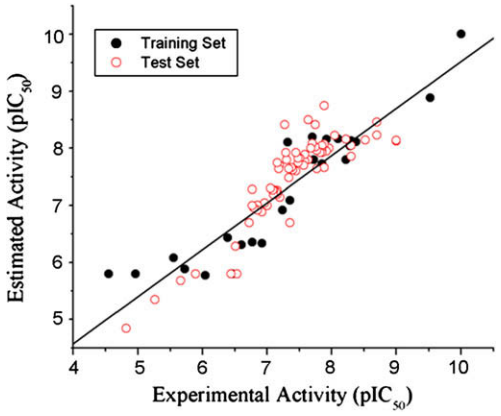

Graph 1. Correlation graph between experimental (pIC_{50}) and Hypo 1-estimated activities (pIC_{50}) of training and test set.

3.2. Docking studies

Initial docking calculations were performed for these 97 known inhibitors to analyze the important interactions between protein and the ligand to generate a structural model for virtual ligand docking (VLS).

All docking calculations were performed using the 'Standard Precision' (SP) mode of GLIDE program and with OPLS-AA 2001 force field. All the compounds in the study were docked in the active site of receptor and calculated the binding interactions. The estimated docking scores (G Score) by the algorithm for these compounds are listed in Table 2. These studies provided insight into interactions that may be important for inhibitor activity by comparing docking simulations of each inhibitor in the Caspase-3.

The docked conformations determined by Glide with the best docking energy for the high active compounds are in the range of −11.35 and for the low active compounds are having in the range of −5.49. In Figure 4a, showing the Glide generated binding pose of highly active compound (62) inside the active of Caspase-3. As depicted from the figure, the compound is showing four hydrogen bond interactions with the atoms active amino acids. The two important hydrogen bond contacts with Arg207, the first hydrogen bond is formed by the backbone CO and NH of the compound (CO···HN, 2.13 Å) and the second hydrogen bond is formed by side chain NH of Arg207 and CO group of the compound (NH···OC, 2.74 Å). Other two crucial hydrogen bond interactions are formed between the compound and the receptor is: NH of indole ring present in Try 214 with CO group of compound (NH···OC, 3.25 Å), backbone NH of Ser209 with carbonyl oxygen of the ligand (NH···OC, 2.62 Å).

All dataset molecules were docked into the active site of Caspase-3, and the correlation was calculated between Glide score and the pIC_{50} by linear regression analysis method. An acceptable correlation coefficient (r) of 0.78 was obtained between experimental pIC_{50} and docking energy (Graph 2).

Table 2
Experimental activity (pIC_{50}) and dock scores obtained by Glide SP of dataset molecules

Compound number	Experimental activity (pIC_{50})	Dock score
sdmol 62	10.000	−11.351
sdmol 20	9.523	−9.037
sdmol 80	9.000	−9.338
sdmol 77	9.000	−8.139
sdmol 82	8.699	−9.822
sdmol 78	8.699	−8.634
sdmol 17	8.523	−8.428
sdmol 11	8.377	−7.868
sdmol 72	8.301	−8.101
sdmol 19	8.301	−8.576
sdmol 15	8.301	−8.952
sdmol 16	8.284	−7.964
sdmol 68	8.222	−8.762
sdmol 60	8.222	−7.410
sdmol 39	8.097	−8.576
sdmol 59	8.046	−7.921
sdmol 58	7.959	−7.096
sdmol 73	7.921	−7.817
sdmol 36	7.921	−7.841
sdmol 61	7.886	−7.416
sdmol 57	7.886	−7.503
sdmol 47	7.886	−6.921
sdmol 71	7.854	−7.341
sdmol 70	7.854	−7.527
sdmol 48	7.854	−7.568
sdmol 44	7.854	−8.354
sdmol 43	7.854	−7.916
sdmol 56	7.824	−7.720
sdmol 64	7.770	−8.030
sdmol 55	7.770	−6.914
sdmol 81	7.745	−7.238
sdmol 34	7.745	−7.365
sdmol 69	7.721	−7.021
sdmol 74	7.699	−7.677
sdmol 67	7.699	−6.484
sdmol 51	7.678	−6.122
sdmol 83	7.638	−6.221
sdmol 46	7.638	−6.272
sdmol 54	7.585	−6.531
sdmol 35	7.585	−7.996
sdmol 85	7.569	−6.208
sdmol 76	7.523	−6.443
sdmol 3	7.509	−6.576
sdmol 97	7.481	−6.771
sdmol 96	7.481	−7.109
sdmol 45	7.481	−5.576
sdmol 86	7.444	−6.094
sdmol 28	7.444	−5.576
sdmol 84	7.398	−6.576
sdmol 53	7.377	−5.576
sdmol 14	7.357	−6.345
sdmol 10	7.357	−6.389
sdmol 79	7.337	−7.072
sdmol 38	7.337	−7.322
sdmol 23	7.319	−5.576
sdmol 65	7.301	−5.576
sdmol 37	7.292	−5.576
sdmol 21	7.276	−7.506
sdmol 95	7.237	−7.263
sdmol 41	7.201	−6.000
sdmol 42	7.194	−6.049
sdmol 63	7.180	−7.031
sdmol 8	7.155	−7.350
sdmol 75	7.155	−6.728
sdmol 66	7.155	−6.855
sdmol 30	7.149	−6.427
sdmol 24	7.143	−6.426
sdmol 40	7.108	−6.300
sdmol 22	7.097	−7.169
sdmol 32	7.086	−6.576
sdmol 25	7.056	−7.223
sdmol 49	7.000	−6.511
sdmol 52	6.959	−6.614
sdmol 50	6.921	−6.342
sdmol 1	6.921	−6.751

Table 2 (*continued*)

Compound number	Experimental activity (pIC_{50})	Dock score
sdmol 31	6.854	−6.855
sdmol 26	6.854	−5.246
sdmol 33	6.796	−5.522
sdmol 5	6.770	−6.220
sdmol 18	6.770	−5.278
sdmol 12	6.770	−6.549
sdmol 29	6.721	−6.188
sdmol 89	6.602	−7.464
sdmol 88	6.532	−7.217
sdmol 27	6.509	−6.018
sdmol 93	6.456	−6.031
sdmol 94	6.441	−6.295
sdmol 9	6.387	−6.187
sdmol 4	6.041	−6.076
sdmol 90	5.889	−5.491
sdmol 7	5.721	−5.679
sdmol 6	5.658	−5.540
sdmol 2	5.553	−5.180
sdmol 13	5.260	−5.702
sdmol 87	4.959	−6.546
sdmol 91	4.814	−4.625

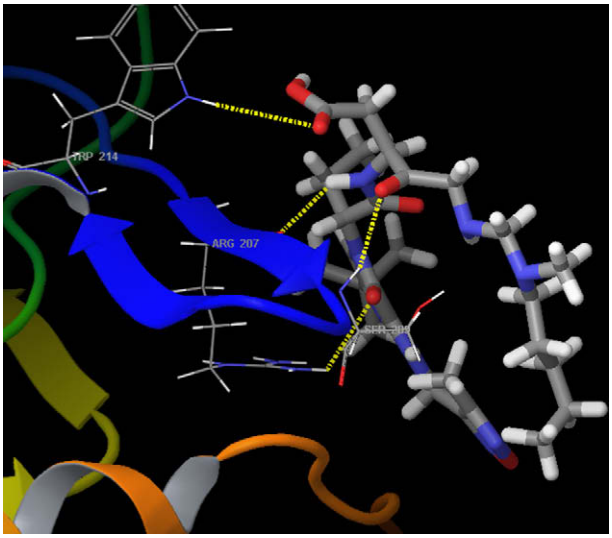

Figure 4. Docked conformation of the most active compound 62 in the active site. Broken lines represent hydrogen bonds.

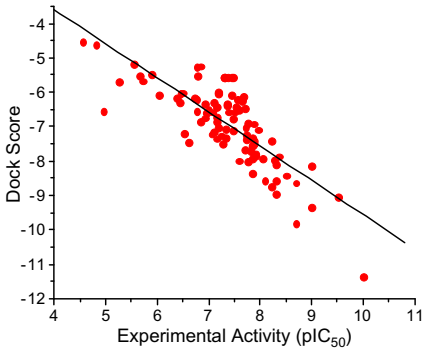

Graph 2. Correlation graph between experimental activity (pIC_{50}) and docking score.

3.3. Virtual screening

The main aim of our study is to identify the non-peptide inhibitors against Caspase-3 for the database. For conducting virtual

screening we used Maybridge database containing 50,000 compounds. Best hypothesis (hypo 1) used as a query, to retrieve the novel and potent candidates from the database. Two thousand five hundred compounds were retrieved as hits and these compounds were further screened for drug like properties using Lipinski rule[29] of 5 as a filter. The remaining molecules were overlaid with the 3D-pharmacophore by using the 'Best Fit' option and the top 200 scored hits were analysed for binding patterns using docking studies. Ten compounds having interactions with important amino acids: Arg207, Try 214, and Ser209 of Caspase-3, were selected for synthesis and biological testing to measure the Caspase-3 inhibitory activity. The binding pose of the AW01208 inside the active site of the Caspase-3 was shown in Figure 5b. The compound is having strong hydrogen bond with the active site amino acid Arg207 (backbone CO with amide NH of the compound with 2.013 Å). We have finished the synthesis and screening for the hit 1 (AW01208) shown in Figure 5a and the synthesis and the inhibitory activity of the hit 1 was evaluated as reported in Section 2.5.

3.4. Biological screening

The first graph with concentration on *x*-axis and fluorescence intensity on *y*-axis in Figure 6 shows induction of non-apoptotic control in SKNH cells shown by increase in fluorescence intensity in comparison to the standard inhibitor used. Further increased concentrations from 0.5 μM to 5 μM of Doxorubicin indicates increased slope values (an average value of 5 experiments in duplicates) with individual concentrations thereby indicating increased levels of apoptosis in the SKNH cell lines further evidenced by increase in fluorescence intensity with strong emission at higher concentrations of Doxorubicin (5 μM).

Plot of fluorescence intensity with respect to variable wavelengths shown in Figure 7. The results showed the maximum fluorescence intensity from 420 to 430 nm for Doxorubicin at 1 μM and 5 μM.

Plot of concentration and fluorescence intensity shown in Figure 8. The various concentrations of the compound AW01208 was taken and fluorescence intensity was studied, the AW01208 showed maximum fluorescence for 10 μM, 50 μM, and 100 μM solutions. The fluorescence was decreasing for increase in concentrations, that is, for 0.5 μM, 1 mM, and 5 mM.

Plot of fluorescence and wavelength shown in Figure 9. The fluorescence of inhibitor compound and standard inhibitor was studied in the range 420–460 nm. The standard inhibitor showed maximum fluorescence at 430–440 nm and the synthesized inhibitor AW01208 of 0.5 μM concentration exhibited maximum fluorescence at 440 nm. The inhibitory effect of Caspase-3 is better

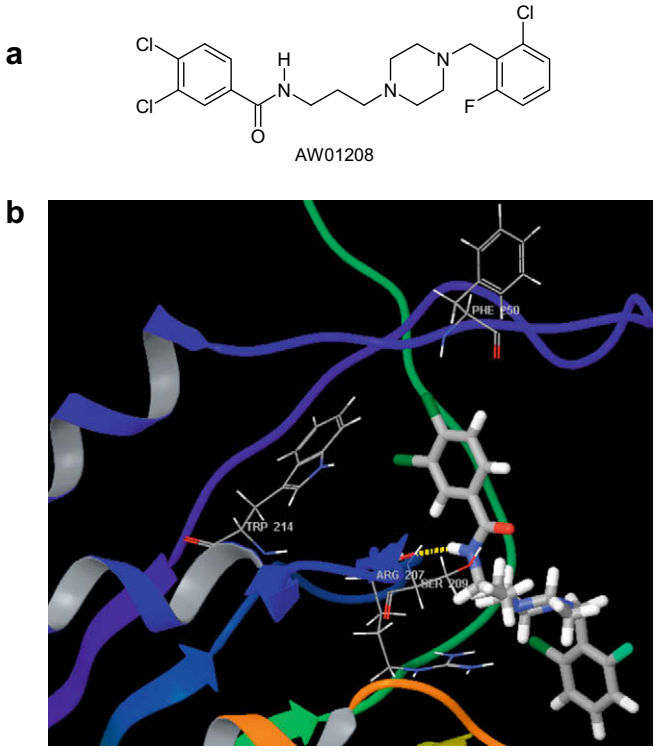

Figure 5. (a) 2D-structure of the virtual screening hit, (b) best docked conformation of the AW01208 in the active site. Broken lines represent hydrogen bonds. Hydrogen bond distances are presented in angstroms (Å).

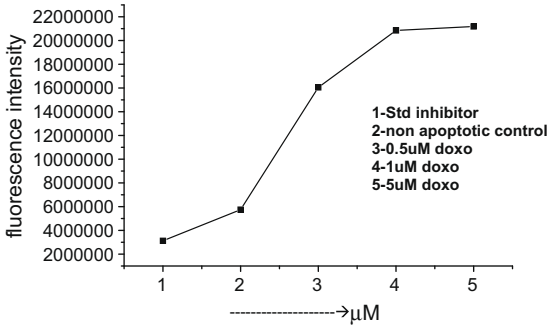

Figure 6. Doxorubicin induced apoptosis in SKNSH cell lines.

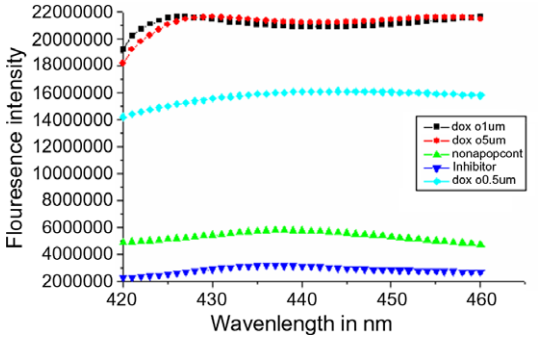

Figure 7. Doxorubicin induced apoptosis in SKNSH cell lines as measured by Caspase-3 activity.

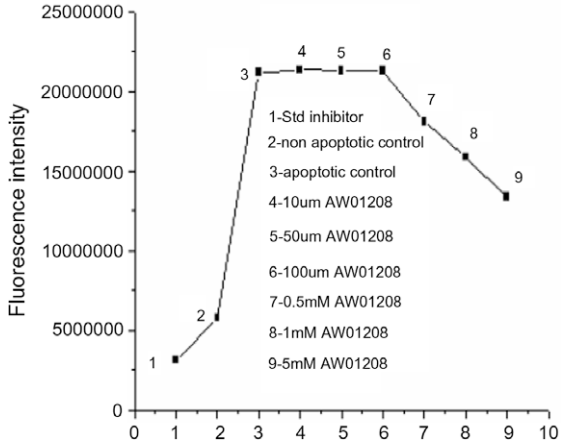

Figure 8. Caspase 3 inhibition by compound AW01208 at various concentrations.

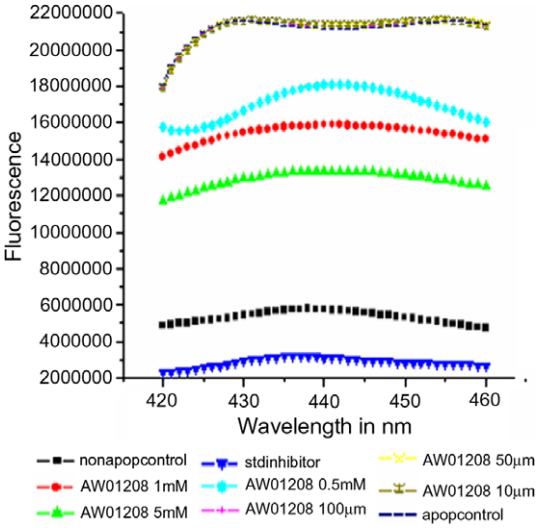

Figure 9. Apoptosis inhibition by AW01208.

evidenced by the decrease in fluorescence intensity when the concentration of the compound is 5 mM which is approximately 50% decrease in intensity with respect to the strong fluorescence emitted by the apoptotic controlled cells but did not show any inhibition at 10 μM. The fluorescence intensity was decreased with increase in concentrations of the lead compound AW01208. It is evident from the graph in Figure 9 that the decrease in fluorescence intensity observed for compound AW01208 at 5 mM concentration and inhibitory effect is approximately 50% when compared to the apoptotic controlled cells. Similar experiments were carried out with Caspase-7 protein and the lead compound AW01208 did not showed much inhibition effect with Caspase-7 protein and hence the experimental results are further not discussed here. From the above biological studies it is evident that the compound AW01208 is a specific inhibitor for Caspase-3 and not for Caspase-7.

The above data obtained shows that the compound AW1208 determined by in silico studies and synthesized in the lab is highly selective. Caspase-3 inhibition was effective then Caspase-7, due to the fact that the receptor sites of Caspase-3 and 7 differ from each other.

4. Conclusion

We have generated ligand based pharmacophore model using 25 diversed compounds. The model consisted of one H-bond acceptor (HBA), one H-bond donor (HBD), and two hydrophobic (HY) features. Further docking studies were performed on the known inhibitors and these results indicated that the amino acids Arg207, Ser209, and Trp214 present in the active site of caspase-3 are important for ligand binding. Using both ligand and structure based models virtual screening was performed against Maybridge database to find the novel non-peptide inhibitors. From this study, we identified compound (AW1208) as a non-peptide inhibitor against Caspase-3.

Supplementary data

Supplementary data associated with this article can be found, in the online version, at doi:10.1016/j.bmc.2009.06.069.

References and notes

1. Jacobson, M. D.; Weil, M.; Raff, M. C. *Cell* **1997**, *88*, 347.
2. Porter, A. G.; Janicke, R. U. *Cell Death Differ.* **1999**, *6*, 99.
3. Nuttall, M. E.; Lee, D.; McLaughlin, B.; Erhardt, J. A. *Drug Discovery Today* **2001**, *6*, 85.
4. Reed, J. C. *Nat. Rev. Drug Disc.* **2002**, *2*, 111.
5. Rodriguez, I.; Matsuura, K.; Ody, C.; Nagata, S.; Vassalli, P. *J. Exp. Med.* **1996**, *184*, 2067.
6. Slee, E. A.; Adrain, C.; Martin, S. J. *J. Biol. Chem* **2000**, *276*, 7320.
7. Denault, J.-B.; Salvesen, G. S. *Chem. Rev.* **2002**, *12*, 4489.
8. Salvesen, G. S.; Dixit, V. M. *Cell* **1997**, *91*, 443–446.
9. Han, B. H.; Xu, D.; Choi, J.; Han, Y.; Xanthoudakis, S.; Roy, S.; Tam, J.; Vaillancourt, J.; Colucci, J.; Siman, R.; Giroux, A.; Robertson, G. S.; Zamboni, R. *J. Biol. Chem.* **2002**, *277*, 30128.
10. Hotchkiss, R. S.; Chang, K. C.; Swanson, P. E.; Tinsley, K. W.; Hui, J. J.; Klender, P.; Xanthoudakis, S.; Roy, S.; Black, C.; Grimm, E.; Aspiotis, R.; Han, Y.; Nicholson, D. W.; Karl, I. E. *Nat. Immunol.* **2000**, *1*, 496–501.
11. Yongxin, H.; Andrem, G.; John, C.; Christopher, I. B.; Daniel, J. M.; Sophie, R.; Steve, X.; John, V.; Dita, M. R.; John, T.; Paul, T.; Donald, W. N.; Robert, J. Z. *Bioorg. Med. Chem. Lett.* **2005**, *15*, 1173.
12. Lee, D.; Long, S. A.; Adams, J. L.; Chan, G.; Vaidya, K. S.; Francis, T. A.; Kikly, K.; Winkler, J. D.; Sung, C. M.; Debouck, C.; Richardson, S.; Levy, M. A.; DeWolf, W. E., Jr.; Keller, P. M.; Tomaszek, T.; Head, M. S.; Ryan, M. D.; Haltiwanger, R. C.; Liang, P. H.; Janson, C. A.; McDevitt, P. J.; Johanson, K.; Concha, N. O.; Chan, W.; Abdel-Meguid, S. S.; Badger, A. M.; Lark, M. W.; Nadeau, D. P.; Suva, L. J.; Gowen, M.; Nuttall, M. E. *J. Biol. Chem.* **2000**, *275*, 16007.
13. Wang, Y.; Guan, L.; Jia, S.; Tseng, B.; Drewe, J.; Cai, S. X. *Bioorg. Med. Chem. Lett.* **2005**, *15*, 1379.
14. Grimm, E. L.; Roy, B.; Aspiotis, R.; Bayly, C. I.; Nicholson, D. W.; Rasper, D. M.; Renaud, J.; Roy, S.; Tam, J.; Tawa, P.; Vaillancourt, J. P.; Xanthoudakis, S.; Zamboni, R. J. *Bioorg. Med. Chem.* **2004**, *12*, 845.
15. Kravchenko, D. V.; Kuzovkova, Y. A.; Kysil, V. M.; Tkachenko, S. E.; Maliarchouk, S.; Okun, I. M.; Balakin, K. V.; Ivachtchenko, A. V. *J. Med. Chem.* **2005**, *48*, 3680.
16. Cerius2 4.11; Accelrys: San Diego, CA, 2005, www.accelrys.com.
17. Stewart, J. J. *J. Comput. Aided Mol. Des.* **1990**, *4*, 1–103.
18. Catalyst 4.11; Accelrys: San Diego, CA, 2005, www.accelrys.com.
19. Smellie, A.; Teig, S. L.; Towbin, P. *J. Comput. Chem.* **1995**, *16*, 171.
20. Smellie, A.; Kahn, S. D.; Teig, S. L. *J. Chem. Inf. Comput. Sci.* **1995**, *35*, 285.
21. Smellie, A.; Kahn, S. D.; Teig, S. L. *J. Chem. Inf. Comput. Sci.* **1995**, *35*, 295.
22. Friesner, R. A.; Banks, J. L.; Murphy, R. B.; Halgren, T. A.; Klicic, J. J.; Mainz, D. T.; Repasky, M. P.; Knoll, E. H.; Shelley, M.; Perry, J. K.; Shaw, D. E.; Francis, P.; Shenkin, P. S. *J. Med. Chem.* **2004**, *47*, 1739.
23. Halgren, T. A.; Murphy, R. B.; Friesner, R. A.; Beard, H. S.; Frye, L. L.; Pollard, W. T.; Banks, J. L. *J. Med. Chem.* **2004**, *47*, 1750.
24. Jorgensen, W. L.; Maxwell, D.; Tirado, R. J. *J. Am. Chem. Soc.* **1996**, *118*, 11225.
25. Maybridge Chemical Company (England); http://www.chem.ac.ru/Chemistry/Databases/MAYBRIDGE.en.html.
26. Michael, J. R.; Stephen, M. H.; Andrej, K.; Robbin, B.; Andrew, T.; Amy, H. N. *J. Med. Chem.* **2001**, *44*, 3175.
27. Chen, Y. H.; Zhang, Y. H.; Zhang, H. J.; Liu, D. Z.; Gu, M.; Li, J. Y.; Wu, F.; Zhu, X. Z.; Li, J.; Nan, F. J. *J. Med. Chem.* **2006**, *49*, 1613.
28. Wenhua, C.; Jun, Z.; Chenbo, Z.; Justin, R.; Zhude, T.; Yunxiang, C.; David, E. R.; Micheal, J. W.; Robert, H. M. *J. Med. Chem.* **2005**, *48*, 7637.
29. Lipinski, C. A. *Adv. Drug Delivery Rev.* **1997**, *23*, 3.